Quantum-mechanical lossless beam splitter: SU(2) symmetry and photon statistics

Richard A. Campos
Columbia Radiation Laboratory, Department of Applied Physics, Columbia University, New York, New York 10027

Bahaa E. A. Saleh
Department of Electrical and Computer Engineering, University of Wisconsin, Madison, Wisconsin 53706

Malvin C. Teich
Columbia Radiation Laboratory, Departments of Electrical Engineering and Applied Physics, Columbia University, New York, New York 10027

(Received 6 June 1988; revised manuscript received 27 March 1989)

For optical homodyning, the matrix representation of a lossless beam splitter belongs to the SU(2) group of unimodular second-order unitary matrices. The connection between this group and the rotation group in three dimensions permits the field density operators at the input and output ports of the beam splitter to be related by means of well-known angular-momentum transformations. This, in turn, provides the joint output photon-number distribution, which may be written as a Fourier series in the relative phase shift imparted by the beam splitter, for a general joint state at its inputs. The series collapses to a single term if one of the input fields is diagonal in the number-state representation. If the inputs to both ports are further restricted to be pure number states, the joint, as well as the marginal photon-number distributions, turn out to be directly proportional to the square of Jacobi polynomials in the beam-splitter transmittance. These photon-number probabilities are invariant to a set of physical and time-reversal symmetries. When one of the input photon-number states is the vacuum, the beam splitter simply deletes photons from the other port in Bernoulli fashion, as if they were classical particles. The output photon number is then described by the binomial distribution. If the inputs at the two ports are different number states, neither of which is the vacuum, the photon-number distribution is expressible in terms of summed and weighted products of the results for photomixing with the vacuum. If the inputs at the two ports are identical number states, and a beam splitter of transmittance $\tau=\frac{1}{2}$ is used, the photon-number distribution assumes a simple but interesting form. It vanishes for odd photon numbers, indicating that the photons assemble in pairs at each output port. Finally, it is shown that homodyning quantum fluctuations can be reduced by using a balanced photomixer for arbitrary input states.

I. INTRODUCTION

The synthesis of various nonclassical states of light in recent years[1,2] has rekindled interest in the lossless beam splitter, not only because of the important role it plays in their coherent detection,[3] but also because the device offers us an opportunity to probe the quantum nature of light by means of simple yet subtle experiments.[4–7]

A number of authors have considered the behavior of the quantum-mechanical beam splitter in the past few years.[8–12] We provide a comprehensive approach that treats the photon statistics arising from the homodyne photomixing of (not necessarily independent) light beams of arbitrary statistical composition. It turns out that important mathematical tools can be borrowed directly from a different, but fully equivalent, physical model: the quantization of angular momentum. In 1952, by employing a two-dimensional boson-operator algebra, and building on a method first used by Jordan,[13] Schwinger reformulated the theory of angular momentum in his now celebrated treatise on the subject.[14] The technique, viewed in reverse, is ideally suited to the beam splitter, which, after all, governs the interaction of two harmonic oscillators. Schwinger's formalism was recently considered by Yurke *et al.*,[8] who showed that interferometry with beam splitters may be viewed geometrically as abstract rotations of angular momenta on a sphere.

In this paper we elaborate on this theme, carrying over to quantum optics many of the well-established mathematical methods and results from the theory of angular momentum. In Sec. II we address the connection between SU(2) beam-splitter matrices and the rotation group in three dimensions. The beam-splitter unitary operator is readily generated from the standard Euler-angle parametrization of that group. In Sec. III we develop an interference field operator and delineate its contribution to the output photon-number fluctuations. Interference in the photon-number domain is the focus of Sec. IV, where we derive a general formalism for the homodyning of arbitrary states into the beam-splitter input ports and explore the various forms of photon-number interference in the joint photon-number distribution at the beam-splitter output ports. Number-state

homodyning, which forms the backbone of the general theory, is discussed in detail and a number of examples are presented. Section V highlights the general balanced photomixer.

II. THE LOSSLESS BEAM SPLITTER

A. Beam-splitter matrix transformation

As a stepping stone to a more abstract, but useful, formalism of the beam splitter, we first derive the general matrix representation of the device from fundamental principles. We limit our discussion to optical homodyning to capture the essential features of beam-splitter photomixing. The terms homodyne detection, photomixing, and coherent detection are used interchangeably in this paper.

For simplicity, we ignore the effects of polarization mismatch and imperfect beam collimation, since these can be incorporated into the theory *a posteriori* without difficulty. The input and output boson-annihilation operators, at some chosen angular frequency ω (see Fig. 1), are related by

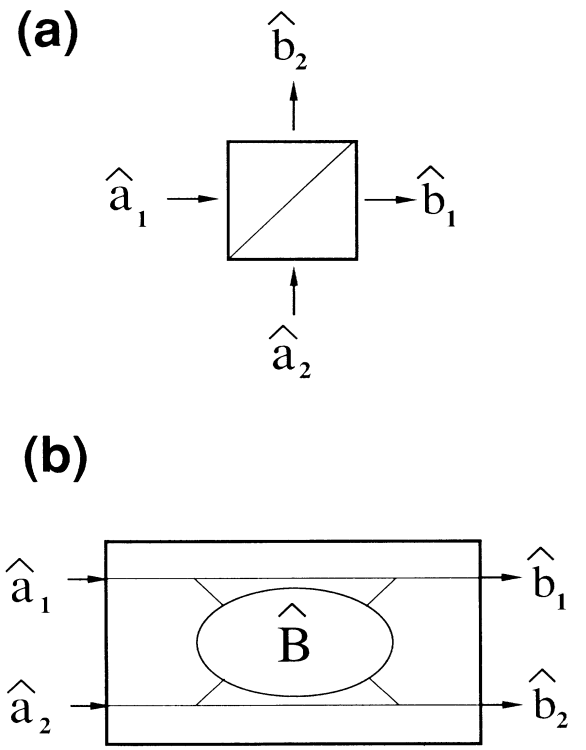

FIG. 1. (a) Beam-splitter geometry and (b) its diagrammatic representation as an optical element with two input ports and two output ports. The transformation is governed by a unitary operator $\hat{B}$, which is equivalent to the standard Euler-angle parametrization of the rotation group. The boson-annihilation operators at the input and output ports are represented by $\hat{a}$ and $\hat{b}$, respectively. The subscripts number the input and output ports.

$$\begin{bmatrix}\hat{b}_1\\ \hat{b}_2\end{bmatrix}=\begin{bmatrix}B_{11} & B_{12}\\ B_{21} & B_{22}\end{bmatrix}\begin{bmatrix}\hat{a}_1\\ \hat{a}_2\end{bmatrix}, \tag{1}$$

where the boson-annihilation operators at the input and output are represented by $\hat{a}$ and $\hat{b}$, respectively. All Hilbert-space operators are denoted by the caret. The subscripts number the input and output ports. The transformation matrix $\underline{B}$ has elements B_{ij}, which are in general complex to allow for field phase shifts at the device, i.e.,

$$B_{ij}=|B_{ij}|e^{i\phi_{ij}},\quad i,j=1,2\ . \tag{2}$$

The preservation of boson commutation relations at the output of the beam splitter, according to

$$[\hat{b}_i,\hat{b}_j^{\dagger}]\equiv\hat{b}_i\hat{b}_j^{\dagger}-\hat{b}_j^{\dagger}\hat{b}_i=\delta_{ij}\ , \tag{3}$$

leads to the conditions

$$|B_{11}|^2+|B_{12}|^2=1\ , \tag{4a}$$

$$|B_{21}|^2+|B_{22}|^2=1\ , \tag{4b}$$

$$B_{11}B_{21}^*+B_{12}B_{22}^*=0\ . \tag{4c}$$

The superposition criteria at the output ports, Eqs. (4a) and (4b), are not independent; indeed, they are coupled via Eq. (4c). This can be seen from the decomposition of the latter into separate conditions on magnitude and phase:

$$|B_{11}|\,|B_{21}|=|B_{12}|\,|B_{22}|\ , \tag{4d}$$

$$\phi_{11}-\phi_{12}=\phi_{21}-\phi_{22}\pm\pi\ . \tag{4e}$$

Combining Eq. (4d) with Eqs. (4a) and (4b), and reexpressing the results in terms of the beam-splitter transmittance τ and its associated reflectance $\rho=(1-\tau)$, leads to

$$|B_{11}|^2=|B_{22}|^2=\tau\equiv\cos^2\theta\ , \tag{5a}$$

$$|B_{12}|^2=|B_{21}|^2=\rho=\sin^2\theta\ . \tag{5b}$$

Thus all of the magnitudes are governed by the single angular parameter

$$\theta=\arccos(\tau^{1/2}),\quad 0\le\theta\le\pi/2\ . \tag{5c}$$

Combining Eq. (4e) with the convenient phase redefinitions

$$\phi_\tau\equiv\tfrac{1}{2}(\phi_{11}-\phi_{22})\ , \tag{6a}$$

$$\phi_\rho\equiv\tfrac{1}{2}(\phi_{12}-\phi_{21}\mp\pi)\ , \tag{6b}$$

$$\phi_0\equiv\tfrac{1}{2}(\phi_{11}+\phi_{22})\ , \tag{6c}$$

allows us to write the most general beam-splitter matrix as

$$\underline{B}=e^{i\phi_0}\begin{bmatrix}\cos\theta e^{i\phi_\tau} & \sin\theta e^{i\phi_\rho}\\ -\sin\theta e^{-i\phi_\rho} & \cos\theta e^{-i\phi_\tau}\end{bmatrix}. \tag{7}$$

Its determinant is

$$\det(\underline{B})=e^{i2\phi_0}\ , \tag{8}$$

so that the transformation is unitary, as one would expect from the preservation of boson commutation rules. The number of photons (and hence the energy) is conserved according to the operator equation

$$\hat{N}_1+\hat{N}_2=\hat{n}_1+\hat{n}_2 \ , \tag{9a}$$

where the output and input number operators are defined as

$$\hat{N}_j=\hat{b}_j^{\dagger}\hat{b}_j, \quad \hat{n}_j=\hat{a}_j^{\dagger}\hat{a}_j, \quad j=1,2 \tag{9b}$$

respectively. The beam splitter is thus properly represented as a lossless optical element.

It is clear that energy conservation alone is not sufficient to determine a standard beam-splitter transformation, as the three independent phases in Eq. (6), as well as the transmittance parameter in Eq. (5), must be specified. It is not surprising, therefore, that a diversity of beam-splitter transformations has appeared in the literature; however, they all belong to the U(2) group of second-order unitary matrices.

On the other hand, by recognizing that the interference effects we seek to describe depend on the relative phases between the two input fields, we may discard, without loss of generality, the global phase factor ϕ_0 of Eq. (6c) by imposing the additional constraint

$$\phi_0=0 \ . \tag{10}$$

This restricts the transformation to the unimodular (i.e., unit determinant) subgroup SU(2), as noted by Yurke *et al.*[8] The simplest nontrivial representation of the subgroup results when the beam splitter imparts no phase shifts onto the input fields,

$$\phi_\tau=\phi_\rho=0 \ . \tag{11a}$$

This reveals the fundamental rotary action of the device,

$$\underline{B}=\begin{bmatrix} \cos\theta & \sin\theta \\ -\sin\theta & \cos\theta \end{bmatrix} . \tag{11b}$$

B. Connection with angular momenta

Although the central results of beam-splitter interferometry can be obtained directly from its governing two-dimensional unitary matrix, as described above, a complementary understanding of the process can be achieved by viewing it in three dimensions. The reduction of the beam-splitter transformation to a matrix with three degrees of freedom is the crucial connection, since the same number of free parameters is required to describe the orientation of a classical solid body in space.[15]

The first step in realizing this correspondence quantum mechanically is to use Schwinger's relations to cast the two-dimensional harmonic oscillator in terms of an angular-momentum system normalized to $\hbar$,[14]

$$\hat{L}_1=\tfrac{1}{2}(\hat{a}_1^{\dagger}\hat{a}_2+\hat{a}_2^{\dagger}\hat{a}_1) \ , \tag{12a}$$

$$\hat{L}_2=\frac{1}{2i}(\hat{a}_1^{\dagger}\hat{a}_2-\hat{a}_2^{\dagger}\hat{a}_1) \ , \tag{12b}$$

$$\hat{L}_3=\tfrac{1}{2}(\hat{a}_1^{\dagger}\hat{a}_1-\hat{a}_2^{\dagger}\hat{a}_2) \ . \tag{12c}$$

As can be verified, these satisfy the standard commutator algebra

$$[\hat{L}_i,\hat{L}_j]=i\epsilon_{ijk}\hat{L}_k \ . \tag{13}$$

The Levi-Cività tensor ϵ_{ijk} is equal to $+1$ and -1 for even and odd permutations of its indices, respectively, and zero otherwise.

The square, and projection, of the angular momentum are related to the boson number operators via

$$\hat{L}^2\equiv\sum_{j=1}^{3}\hat{L}_j^2=\hat{l}(\hat{l}+1), \quad \hat{L}_3\equiv\hat{m} \ , \tag{14a}$$

$$\hat{l}\equiv\tfrac{1}{2}(\hat{n}_1+\hat{n}_2), \quad \hat{m}\equiv\tfrac{1}{2}(\hat{n}_1-\hat{n}_2) \ . \tag{14b}$$

Since the expectation of $\hat{l}$ in a general state measures the mean total number of photons at the input ports, the confinement of the angular momentum to a sphere in the Schwinger paradigm is equivalent to the conservation of average energy in the system. The mean photon-number difference, on the other hand, represents the average input projection of angular momentum. For number states at the input ports, the standard inequality $-l\le m\le l$ assures a degeneracy of $2l+1$ input configurations when the system contains $2l=n_1+n_2$ photons. This is shown in Fig. 2(a) for $l=1$.

Let us consider a transformation of the Schwinger angular momenta via a unitary operator $\hat{B}(\Phi,\Theta,\Psi)$ according to the similarity operation,

$$\hat{L}'_j=\hat{B}(\Phi,\Theta,\Psi)\hat{L}_j\hat{B}^{\dagger}(\Phi,\Theta,\Psi), \quad j=1,2,3 \ . \tag{15a}$$

This causes the vector to rotate on the angular-momentum sphere to a new position that depends on the three angular parameters (Φ,Θ,Ψ). The primed angular momenta can be written in the form of Eq. (12),

$$\hat{L}'_1=\tfrac{1}{2}(\hat{b}_1^{\dagger}\hat{b}_2+\hat{b}_2^{\dagger}\hat{b}_1) \ , \tag{15b}$$

$$\hat{L}'_2=\frac{1}{2i}(\hat{b}_1^{\dagger}\hat{b}_2-\hat{b}_2^{\dagger}\hat{b}_1) \ , \tag{15c}$$

$$\hat{L}'_3=\tfrac{1}{2}(\hat{b}_1^{\dagger}\hat{b}_1-\hat{b}_2^{\dagger}\hat{b}_2) \ , \tag{15d}$$

provided that the new annihilation operators are obtained in a similar fashion from

$$\hat{b}_j=\hat{B}(\Phi,\Theta,\Psi)\hat{a}_j\hat{B}^{\dagger}(\Phi,\Theta,\Psi), \quad j=1,2 \ . \tag{16}$$

The unitarity of $\hat{B}(\Phi,\Theta,\Psi)$ preserves the commutator algebra of Eq. (13), thereby ensuring a canonical transformation of the annihilation operators. The $\hat{b}$-field operators, which have been discussed by Titulaer and Glauber,[16] therefore generate their own set of number states from the vacuum:

$$|N_j\rangle=\frac{(\hat{b}_j^{\dagger})^{N_j}}{(N_j!)^{1/2}}|0\rangle \ . \tag{17}$$

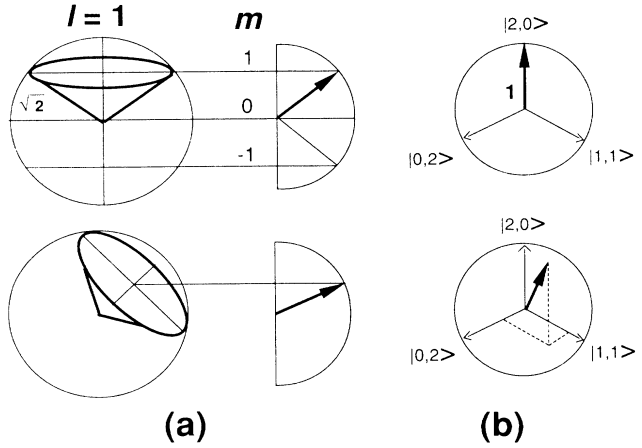

FIG. 2. Two equivalent geometric views of the unitary beam-splitter transformation when n_1 and n_2 photons are incident on the device. (a) An angular-momentum vector is represented quantum mechanically by a cone, as its projection along the polar axis is well specified, but the remaining two orthogonal components are uncertain. For fixed energy $l=\frac{1}{2}(n_1+n_2)$, there are $(2l+1)$ possible values of the polar component $m=\frac{1}{2}(n_1-n_2)$ of angular momentum, indicated in the diagram by three possible values of m for $l=1$. The beam-splitter operator rotates any input cone on the Bloch sphere of radius $[l(l+1)]^{1/2}$. (b) In the complementary view, the same operator rotates the unit-magnitude state vector in a $(2l+1)$-dimensional Hilbert space. For $l=1$, this is just the unit sphere, as shown.

The transformation operator $\hat{B}(\Phi,\Theta,\Psi)$ is thus sufficient to characterize the beam splitter. According to the theory of angular momentum, this operator is just the standard representation of the rotation [SO(3), or special orthogonal] group in three dimensions,[17–19]

$$\hat{B}(\Phi,\Theta,\Psi)=e^{-i\Phi\hat{L}_3}e^{-i\Theta\hat{L}_2}e^{-i\Psi\hat{L}_3}\ , \tag{18}$$

where the parameters (Φ,Θ,Ψ) are quantum-mechanical counterparts to the classical Euler angles. Each exponentiated angular-momentum operator generates a new spatial orientation by implementing rotations about the axis corresponding to its label. For example,[8,20]

$$e^{-i\Theta\hat{L}_2}\begin{bmatrix}\hat{L}_1\\ \hat{L}_2\\ \hat{L}_3\end{bmatrix}e^{i\Theta\hat{L}_2}=\begin{bmatrix}\cos\Theta & 0 & -\sin\Theta\\ 0 & 1 & 0\\ \sin\Theta & 0 & \cos\Theta\end{bmatrix}\begin{bmatrix}\hat{L}_1\\ \hat{L}_2\\ \hat{L}_3\end{bmatrix}\ , \tag{19a}$$

$$e^{-i\Phi\hat{L}_3}\begin{bmatrix}\hat{L}_1\\ \hat{L}_2\\ \hat{L}_3\end{bmatrix}e^{i\Phi\hat{L}_3}=\begin{bmatrix}\cos\Phi & \sin\Phi & 0\\ -\sin\Phi & \cos\Phi & 0\\ 0 & 0 & 1\end{bmatrix}\begin{bmatrix}\hat{L}_1\\ \hat{L}_2\\ \hat{L}_3\end{bmatrix}\ . \tag{19b}$$

In accordance with Schwinger's formalism, this implies that $\hat{L}_2$ and $\hat{L}_3$ transform the input boson operators $\hat{a}_1$ and $\hat{a}_2$ according to

$$e^{-i\Theta\hat{L}_2}\begin{bmatrix}\hat{a}_1\\ \hat{a}_2\end{bmatrix}e^{i\Theta\hat{L}_2}=\begin{bmatrix}\cos(\Theta/2) & \sin(\Theta/2)\\ -\sin(\Theta/2) & \cos(\Theta/2)\end{bmatrix}\begin{bmatrix}\hat{a}_1\\ \hat{a}_2\end{bmatrix} \tag{20a}$$

$$e^{-i\Phi\hat{L}_3}\begin{bmatrix}\hat{a}_1\\ \hat{a}_2\end{bmatrix}e^{i\Phi\hat{L}_3}=\begin{bmatrix}e^{i(\Phi/2)} & 0\\ 0 & e^{-i(\Phi/2)}\end{bmatrix}\begin{bmatrix}\hat{a}_1\\ \hat{a}_2\end{bmatrix}\ , \tag{20b}$$

so that the combined phase-shift and rotation effects of $\hat{B}(\Phi,\Theta,\Psi)$ result in the SU(2) matrix

$$\underline{B}=\begin{bmatrix}e^{i(\Psi/2)} & 0\\ 0 & e^{-i(\Psi/2)}\end{bmatrix}\begin{bmatrix}\cos(\Theta/2) & \sin(\Theta/2)\\ -\sin(\Theta/2) & \cos(\Theta/2)\end{bmatrix}\begin{bmatrix}e^{i(\Phi/2)} & 0\\ 0 & e^{-i(\Phi/2)}\end{bmatrix}$$
$$=\begin{bmatrix}\cos(\Theta/2)e^{i[(\Psi+\Phi)/2]} & \sin(\Theta/2)e^{i[(\Psi-\Phi)/2]}\\ -\sin(\Theta/2)e^{-i[(\Psi-\Phi)/2]} & \cos(\Theta/2)e^{-i[(\Psi+\Phi)/2]}\end{bmatrix}\ . \tag{21}$$

Comparison with the desired solution represented in Eqs. (7) and (10), provides the association of Euler angles to beam-splitter parameters:

$$\theta=\tfrac{1}{2}\Theta,\quad \phi_\tau=\tfrac{1}{2}(\Psi+\Phi),\quad \phi_\rho=\tfrac{1}{2}(\Psi-\Phi)\ . \tag{22}$$

With the help of Eqs. (5c) and (18), we readily obtain the general SU(2) beam-splitter operator

$$\hat{B}(\tau,\phi_\tau,\phi_\rho)=e^{-i(\phi_\tau-\phi_\rho)\hat{L}_3}e^{-i2\arccos(\tau^{1/2})\hat{L}_2}e^{-i(\phi_\tau+\phi_\rho)\hat{L}_3}\ . \tag{23}$$

If we now consider the raising and lowering angular-momentum operators

$$\hat{L}_\pm=\hat{L}_1\pm i\hat{L}_2=(\hat{a}_1^\dagger\hat{a}_2,\hat{a}_2^\dagger\hat{a}_1)\ , \tag{24a}$$

so named because they raise and lower the projection m of angular momentum by one unit for states with well-defined projections,

$$\hat{L}_\pm|l,m\rangle=[l(l+1)-m(m\pm1)]^{1/2}|l,m\pm1\rangle\ , \tag{24b}$$

we can then rewrite Eq. (23) with Eqs. (19b) and (24a) as

$$\hat{B}(\tau,\phi_\tau,\phi_\rho)=\hat{D}^\dagger(\zeta)e^{-i2\phi_\tau\hat{L}_3}\ , \tag{25a}$$

where

$$\hat{D}(\zeta)\equiv e^{\zeta\hat{L}_+-\zeta^*\hat{L}_-},\quad \zeta\equiv\arccos(\tau^{1/2})e^{-i(\phi_\tau-\phi_\rho)}\ . \tag{25b}$$

Equation (25b) is the two-mode mixing operator of Schumaker,[21] which was obtained in the context of the beam splitter by Prasad *et al.*[9]

As an alternative approach to the beam-splitter transformation outlined so far we consider the effect of the beam splitter operator on the joint input state, as opposed to its effect on the explicit field operators themselves:

$$|\Psi_{\rm out}\rangle=\hat{B}^{\dagger}(\tau,\phi_\tau,\phi_\rho)|\Psi_{\rm in}\rangle\ , \tag{26a}$$

$$\hat{\rho}_{\rm out}=\hat{B}^{\dagger}(\tau,\phi_\tau,\phi_\rho)\hat{\rho}_{\rm in}\hat{B}(\tau,\phi_\tau,\phi_\rho)\ . \tag{26b}$$

The output density operator $\hat{\rho}_{\rm out}=|\Psi_{\rm out}\rangle\langle\Psi_{\rm out}|$ for pure states. For such states, in place of rotating the "vector" associated with the angular-momentum operators, we instead rotate the "coordinate system" associated with the Hilbert space, as illustrated in Fig. 2(b). This result will prove useful in Sec. IV, where we consider how the beam splitter alters the photon statistics of the input fields.

III. PHOTON-NUMBER MEAN AND VARIANCE

Before examining the full photon-number distribution, it is useful to calculate the photon-number mean and variance at the beam-splitter output ports. The superposition annihilation operators at the beam-splitter output ports are, from Eqs. (5), (7), and (10),

$$\hat{b}_1=\tau^{1/2}e^{i\phi_\tau}\hat{a}_1+(1-\tau)^{1/2}e^{i\phi_\rho}\hat{a}_2\ , \tag{27a}$$

$$\hat{b}_2=-(1-\tau)^{1/2}e^{-i\phi_\rho}\hat{a}_1+\tau^{1/2}e^{-i\phi_\tau}\hat{a}_2\ . \tag{27b}$$

From Eq. (9b), the output number operators are therefore

$$\hat{N}_1=\tau\hat{n}_1+(1-\tau)\hat{n}_2+2[\tau(1-\tau)]^{1/2}\hat{I}\ , \tag{28a}$$

$$\hat{N}_2=(1-\tau)\hat{n}_1+\tau\hat{n}_2-2[\tau(1-\tau)]^{1/2}\hat{I}\ , \tag{28b}$$

where $\hat{I}$ is an interference operator defined in accordance with Eq. (24a) by

$$\begin{aligned}\hat{I}&\equiv\tfrac{1}{2}(\hat{L}_+e^{-i(\phi_\tau-\phi_\rho)}+\hat{L}_-e^{i(\phi_\tau-\phi_\rho)})\\&=\hat{L}_1\cos(\phi_\tau-\phi_\rho)+\hat{L}_2\sin(\phi_\tau-\phi_\rho)\ .\end{aligned} \tag{29}$$

The latter expression is in the form of a field whose quadratures are the first two Schwinger angular momenta.

A. Mean

The intensity at the output ports is proportional to

$$\langle\hat{N}_1\rangle=\tau\langle\hat{n}_1\rangle+(1-\tau)\langle\hat{n}_2\rangle+2[\tau(1-\tau)]^{1/2}\langle\hat{I}\rangle\ , \tag{30a}$$

$$\langle\hat{N}_2\rangle=(1-\tau)\langle\hat{n}_1\rangle+\tau\langle\hat{n}_2\rangle-2[\tau(1-\tau)]^{1/2}\langle\hat{I}\rangle\ . \tag{30b}$$

For example, if coherent states[22] with parameters

$$\alpha_j=|\alpha_j|e^{i\phi_j},\quad j=1,2 \tag{31a}$$

are presented at the input ports,

$$\langle\alpha_1,\alpha_2|\hat{I}|\alpha_1,\alpha_2\rangle=|\alpha_1|\,|\alpha_2|\cos(\phi_1-\phi_2+\phi_\tau-\phi_\rho)\ , \tag{31b}$$

so that the classical first-order interference pattern is recovered. First-order interference is not present in the number states,[23] on the other hand, since all odd moments of the interference operator vanish,

$$\langle n_1,n_2|\hat{I}^{2k+1}|n_1,n_2\rangle=0,\quad \text{all } k\ . \tag{32}$$

More generally, states whose density operator is diagonal in the number-state representation will also lack first-order interference.

B. Variance

The variance of the output photon number may be obtained by using an operator identity for arbitrary $\hat{X}$ and $\hat{Y}$,

$$\begin{aligned}\mathrm{var}(\hat{X}+\hat{Y})&=\langle(\hat{X}+\hat{Y})^2\rangle-\langle(\hat{X}+\hat{Y})\rangle^2\\&=\mathrm{var}(\hat{X})+\mathrm{var}(\hat{Y})+\Xi(\hat{X},\hat{Y})\ .\end{aligned} \tag{33}$$

Here $\Xi(\hat{X},\hat{Y})$ contains the quantum covariances,

$$\Xi(\hat{X},\hat{Y})\equiv\mathrm{cov}(\hat{X},\hat{Y})+\mathrm{cov}(\hat{Y},\hat{X})\ , \tag{34a}$$

which are defined as in classical statistics

$$\mathrm{cov}(\hat{X},\hat{Y})\equiv\langle\hat{X}\,\hat{Y}\rangle-\langle\hat{X}\rangle\langle\hat{Y}\rangle\ . \tag{34b}$$

Straightforward repeated applications of Eq. (33) to Eq. (28), together with Eq. (34), readily provide

$$\begin{aligned}\mathrm{var}(\hat{N}_1)=&[\tau^2\mathrm{var}(\hat{n}_1)+(1-\tau)^2\mathrm{var}(\hat{n}_2)+2\tau(1-\tau)\mathrm{cov}(\hat{n}_1,\hat{n}_2)]\\&+[4\tau(1-\tau)\mathrm{var}(\hat{I})+2\tau^{3/2}(1-\tau)^{1/2}\Xi(\hat{n}_1,\hat{I})+2(1-\tau)^{3/2}\tau^{1/2}\Xi(\hat{n}_2,\hat{I})]\ ,\end{aligned} \tag{35a}$$

$$\begin{aligned}\mathrm{var}(\hat{N}_2)=&[(1-\tau)^2\mathrm{var}(\hat{n}_1)+\tau^2\mathrm{var}(\hat{n}_2)+2\tau(1-\tau)\mathrm{cov}(\hat{n}_1,\hat{n}_2)]\\&+[4\tau(1-\tau)\mathrm{var}(\hat{I})-2(1-\tau)^{3/2}\tau^{1/2}\Xi(\hat{n}_1,\hat{I})-2\tau^{3/2}(1-\tau)^{1/2}\Xi(\hat{n}_2,\hat{I})]\ .\end{aligned} \tag{35b}$$

The first three terms of these equations arise from the quantum-statistical fluctuations inherent in the fields prior to photomixing.

If these input fields are independent, the overall input density operator $\hat{\rho}_{\rm in}$ can be factored into a product of the density operators at each of the input ports,

$$\hat{\rho}_{\rm in}=\hat{\rho}_1\otimes\hat{\rho}_2\ , \tag{36a}$$

so that the number-operator covariance vanishes

$$\mathrm{cov}(\hat{n}_1,\hat{n}_2)=0\ . \tag{36b}$$

The statistical fluctuations associated with the remaining

three terms are attributable to the beam splitter. The first of these represents fluctuations arising from the interference operator, while the last two terms of Eqs. (35a) and (35b) contain correlations among the number operators and the interference operator. When these correlations vanish, the input number operators and the interference operator contribute independently to the output photon-number fluctuations.

Using Eqs. (29) and (33), we can expand the variance of the interference operator in terms of the raising and lowering operators of Eq. (24a) as

$$\mathrm{var}(\hat{I})=\tfrac{1}{4}[\langle \hat{n}_1\rangle+\langle \hat{n}_2\rangle+2\langle \hat{n}_1\hat{n}_2\rangle-2\langle \hat{L}_+\rangle\langle \hat{L}_-\rangle +\mathrm{var}(\hat{L}_+)e^{-i2(\phi_\tau-\phi_\rho)}+\mathrm{var}(\hat{L}_-)e^{i2(\phi_\tau-\phi_\rho)}] . \tag{37}$$

With coherent states at the inputs, for example,

$$\mathrm{var}(\hat{I})=\tfrac{1}{4}(|\alpha_1|^2+|\alpha_2|^2) , \tag{38}$$

as only the first two terms of Eq. (37) contribute. On the other hand, if the input fields are pure number states,

$$\mathrm{var}(\hat{I})=\tfrac{1}{4}(n_1+n_2+2n_1n_2) , \tag{39}$$

which contains an additional product term that contributes significantly to the output photon-number fluctuations.

The correlations between the number operators and the interference operator vanish for both the coherent and number states. Thus, from Eqs. (35), (38), and (39), the overall fluctuations of the output number operators for the coherent states are

$$\mathrm{var}(\hat{N}_1)=\tau|\alpha_1|^2+(1-\tau)|\alpha_2|^2 \tag{40a}$$

$$\mathrm{var}(\hat{N}_2)=(1-\tau)|\alpha_1|^2+\tau|\alpha_2|^2 , \tag{40b}$$

whereas for the number states

$$\mathrm{var}(\hat{N}_1)=\mathrm{var}(\hat{N}_2)=\tau(1-\tau)(n_1+n_2+2n_1n_2) . \tag{41}$$

IV. PHOTON-NUMBER PROBABILITY DISTRIBUTIONS

A. General input state

Having evaluated the first two statistical moments of the photon number at the beam-splitter output, we now turn to the full probability distribution. We represent the general joint input density operator in the number-state representation as

$$\hat{\rho}_{\mathrm{in}}=\sum_{n_1,n_2=0}^{\infty}\sum_{n_1',n_2'=0}^{\infty}\rho_{\mathrm{in}}(n_1,n_2;n_1',n_2')|n_1,n_2\rangle\langle n_1',n_2'| , \tag{42}$$

where the primed variables permit the possibility of off-diagonal elements in this operator. Utilizing Eq. (26b), we write the joint density operator at the output of the beam splitter in the form

$$\hat{\rho}_{\mathrm{out}}=\sum_{N_1,N_2=0}^{\infty}\sum_{N_1',N_2'=0}^{\infty}\rho_{\mathrm{out}}(N_1,N_2;N_1',N_2')\times|N_1,N_2\rangle\langle N_1',N_2'| . \tag{43a}$$

Here N_1 and N_2 characterize the basis states at output ports 1 and 2, respectively. The matrix elements of this density operator are given by

$$\rho_{\mathrm{out}}(N_1,N_2;N_1',N_2')=\sum_{n_1,n_2}\sum_{n_1',n_2'}B_{N_1,N_2}^{(n_1,n_2)}(B_{N_1',N_2'}^{(n_1',n_2')})^*\rho_{\mathrm{in}}(n_1,n_2;n_1',n_2') . \tag{43b}$$

The complex B coefficients depend on the beam-splitter parameters τ, ϕ_τ, and ϕ_ρ, and are related to the beam-splitter operator of Eq. (23) by

$$B_{N_1,N_2}^{(n_1,n_2)}\equiv\langle N_1,N_2|\hat{B}^\dagger(\tau,\phi_\tau,\phi_\rho)|n_1,n_2\rangle =R_{N_1,N_2}^{(n_1,n_2)}e^{i[\phi_\tau(N_1-n_2)+\phi_\rho(N_1-n_1)]} . \tag{43c}$$

The magnitude of these coefficients is provided by the matrix element of the exponentiated angular-momentum $\hat{L}_2$,

$$R_{N_1,N_2}^{(n_1,n_2)}\equiv|B_{N_1,N_2}^{(n_1,n_2)}| =\langle N_1,N_2|e^{i2\arccos(\tau^{1/2})\hat{L}_2}|n_1,n_2\rangle . \tag{43d}$$

It represents the output photon-number probability amplitude for input number states, and will subsequently be evaluated. Conservation of energy is mandated by the SU(2) symmetry of the beam-splitter operator for each matrix element of Eq. (43c) in accordance with

$$N_1+N_2=n_1+n_2 . \tag{43e}$$

For fixed N_1 and N_2, we sum over the range $n_1=(0,\ldots,N_1+N_2)$ in Eq. (43b). A second sum over n_2 is therefore not necessary, as $n_2=N_1+N_2-n_1$. The same applies to the primed variables.

The joint probability of observing N_1 and N_2 photons at the first and second output ports, respectively, is given by the diagonal elements of the output density operator of Eq. (43a),

$$P_{\mathrm{out}}(N_1,N_2)\equiv\langle N_1,N_2|\hat{\rho}_{\mathrm{out}}|N_1,N_2\rangle =\sum_{n_1=0}^{N_1+N_2}\sum_{n_1'=0}^{N_1+N_2}B_{N_1,N_2}^{(n_1,n_2)}(B_{N_1,N_2}^{(n_1',n_2')})^*\times\rho_{\mathrm{in}}(n_1,n_2;n_1',n_2') . \tag{44a}$$

The marginal photon-number output distributions are therefore given by

$$P_{\text{out}}(N_1)=\sum_{N_2=0}^{\infty} P_{\text{out}}(N_1,N_2)\ , \tag{44b}$$

$$P_{\text{out}}(N_2)=\sum_{N_1=0}^{\infty} P_{\text{out}}(N_1,N_2)\ . \tag{44c}$$

We can recast Eq. (44a), with the help of Eqs. (43c) and (43e), as

$$P_{\text{out}}(N_1,N_2)=\sum_{k=-(N_1+N_2)}^{N_1+N_2}\gamma_k(N_1,N_2)e^{-ik(\phi_\tau-\phi_\rho)}\ , \tag{45a}$$

which is a restricted Fourier series in the relative phase $(\phi_\tau-\phi_\rho)$ imparted by the beam splitter. The index k of this series is given by

$$k\equiv n_1'-n_1=n_2-n_2'\ . \tag{45b}$$

The complex expansion coefficients $\gamma_k(N_1,N_2)$ in Eq. (45a) are

$$\gamma_k(N_1,N_2)=\sum_{n_1=0}^{N_1+N_2} R_{N_1,N_2}^{(n_1,n_2)}R_{N_1,N_2}^{(n_1+k,n_2-k)}\times\rho_{\text{in}}(n_1,n_2;n_1+k,n_2-k)\ . \tag{45c}$$

If the general joint input state is pure, then the density operator is of the form

$$\hat{\rho}_{\text{in}}=|\Psi_{\text{in}}\rangle\langle\Psi_{\text{in}}|\ ,$$

$$|\Psi_{\text{in}}\rangle=\sum_{n_1,n_2=0}^{\infty} C_{\text{in}}(n_1,n_2)|n_1,n_2\rangle\ , \tag{46a}$$

and the matrix elements of the input density operator are factorizable according to

$$\rho_{\text{in}}(n_1,n_2;n_1',n_2')=C_{\text{in}}(n_1,n_2)C_{\text{in}}^{*}(n_1',n_2')\ . \tag{46b}$$

Equation (45c) can now be written

$$\gamma_k(N_1,N_2)=\sum_{n_1=0}^{N_1+N_2}\Gamma_{N_1,N_2}(n_1,n_2)\times\Gamma_{N_1,N_2}^{*}(n_1+k,n_2-k)\ , \tag{46c}$$

where

$$\Gamma_{N_1,N_2}(n_1,n_2)=R_{N_1,N_2}^{(n_1,n_2)}C_{\text{in}}(n_1,n_2)\ . \tag{46d}$$

If the joint input density operator is diagonal in the number-state representation, then by Eq. (45b) the joint output probabilities are given by the $k=0$ term of the Fourier series. They then can be recast in the appealing form

$$P_{\text{out}}(N_1,N_2)=\gamma_0(N_1,N_2)=\sum_{n_1=0}^{N_1+N_2}P_{\text{out}}(N_1,N_2|n_1,n_2)P_{\text{in}}(n_1,n_2)\ , \tag{47a}$$

where the conditional and joint probabilities in the sum are defined by

$$P_{\text{out}}(N_1,N_2|n_1,n_2)=(R_{N_1,N_2}^{(n_1,n_2)})^2\ , \tag{47b}$$

$$P_{\text{in}}(n_1,n_2)=\rho_{\text{in}}(n_1,n_2;n_1,n_2)\ . \tag{47c}$$

For pure number states at the input ports, the joint output photon-number probabilities are given by Eq. (47b).

B. Number-state homodyning

We choose now to focus on the output photon-number probability amplitude R of Eq. (43d), which describes all homodyning experiments with the pure number states. The joint photon-number distribution at the output of the beam splitter, arising from number states at the input ports, is given simply by the square of this amplitude function, as Eq. (47b) indicates. Since the system has a well-defined input energy, the conservation criterion of Eq. (43e) renders the sums in Eqs. (44b) and (44c) redundant. The joint and marginal photon-number distributions are then equivalent.

Expanding the input ket in Eq. (43d) in terms of the vacuum, and using the unitarity of the exponentiated angular momentum $\hat{L}_2$, we arrive at

$$R_{N_1,N_2}^{(n_1,n_2)}=\left\langle N_1,N_2\left|\frac{[\tau^{1/2}\hat{a}_1^{\dagger}-(1-\tau)^{1/2}\hat{a}_2^{\dagger}]^{n_1}[(1-\tau)^{1/2}\hat{a}_1^{\dagger}+\tau^{1/2}\hat{a}_2^{\dagger}]^{n_2}}{(n_1!n_2!)^{1/2}}\right|0,0\right\rangle$$

$$=\sum_{k=0}^{n_1}(-1)^{n_1-k}\left[\binom{N_1}{k}\binom{N_2}{n_1-k}\right]^{1/2}\left[\binom{n_1}{k}\tau^{k}(1-\tau)^{n_1-k}\binom{n_2}{N_1-k}(1-\tau)^{N_1-k}\tau^{n_2-(N_1-k)}\right]^{1/2}\ , \tag{48a}$$

where conservation of energy provides $N_2=n_1+n_2-N_1$, and $\binom{n}{k}$ denotes the binomial coefficients $n!/(n-k)!k!$.

The corresponding expression for Eq. (48a) in the angular-momentum domain is well known, having been studied in connection with SU(2) representation functions.[14,18,19] All of its properties can therefore be used, in conjunction with the Schwinger formalism, to provide insights into the behavior of Eq. (48a). Indeed, R can be expressed in terms of the Jacobi polynomials $P_n^{(\alpha,\beta)}(x)$, or generalized spherical functions,[24,25]

$$R_{N_1,N_2}^{(n_1,n_2)} = \left[\frac{N_1!N_2!}{n_1!n_2!} \tau^{N_1-n_2}(1-\tau)^{N_1-n_1} \right]^{1/2} P_{N_2}^{(N_1-n_1,N_1-n_2)}(2\tau-1), \quad N_1 \geq n_1, n_2$$

$$= (-1)^{N_2} \left[\frac{N_1!}{N_2!n_1!n_2!} \tau^{-(N_1-n_2)}(1-\tau)^{-(N_1-n_1)} \right]^{1/2} \left[\frac{d}{d\tau} \right]^{N_2} [\tau^{n_1}(1-\tau)^{n_2}] . \tag{48b}$$

In the last step we have employed the standard Rodrigues formula for the Jacobi polynomials

$$P_n^{(\alpha,\beta)}(x) = \frac{(-1)^n}{2^n n!}(1-x)^{-\alpha}(1+x)^{-\beta} \times \left[\frac{d}{dx} \right]^n [(1-x)^{n+\alpha}(1+x)^{n+\beta}] ,$$

$$\alpha,\beta > -1, \quad -1 \leq x \leq 1 . \tag{48c}$$

According to Eq. (47b), the photon-number probabilities at the output ports are just the square of Eq. (48b), and therefore depend on the square of the Jacobi polynomials

$$P_{\text{out}}(N_1,N_2|n_1,n_2) = \frac{N_1!N_2!}{n_1!n_2!} \tau^{N_1-n_2}(1-\tau)^{N_1-n_1} \times \left[P_{N_2}^{(N_1-n_1,N_1-n_2)}(2\tau-1) \right]^2 ,$$

$$N_1 \geq n_1, n_2 . \tag{48d}$$

The auxiliary requirements $N_1 \geq n_1$ ($\alpha > -1$) and $N_1 \geq n_2$ ($\beta > -1$) ensure the orthogonality of the Jacobi polynomials on the interval $0 \leq \tau \leq 1$ ($-1 \leq x \leq 1$). Certain beam-splitter physical symmetries must therefore exist in order for there to be a complete correspondence between the photon-number output probabilities and the Jacobi polynomials.

C. Symmetries of the output probabilities

The unitarity of the beam-splitter operator, and the special rotation property

$$e^{i\pi\hat{L}_2}|n_1,n_2\rangle = (-1)^{n_1}|n_2,n_1\rangle , \tag{49}$$

are sufficient to provide the beam-splitter probability-amplitude symmetries[14,18,19]

$$R_{N_1,N_2}^{(n_1,n_2)} = (-1)^{N_1-n_1} R_{n_1,n_2}^{(N_1,N_2)} \quad (N_1 < n_1, \ N_1 \geq n_2) , \tag{50a}$$

$$R_{N_1,N_2}^{(n_1,n_2)} = R_{n_2,n_1}^{(N_2,N_1)} \quad (N_1 \geq n_1, \ N_1 < n_2) , \tag{50b}$$

$$R_{N_1,N_2}^{(n_1,n_2)} = (-1)^{N_1-n_1} R_{N_2,N_1}^{(n_2,n_1)} \quad (N_1 < n_1, \ N_1 < n_2) . \tag{50c}$$

With the help of Eq. (47b), these imply that, for each beam-splitter configuration with the number states, there exists three other configurations that yield an identical output probability, i.e.,

$$P_{\text{out}}(N_1,N_2|n_1,n_2) = P_{\text{out}}(n_1,n_2|N_1,N_2) = P_{\text{out}}(n_2,n_1|N_2,N_1) = P_{\text{out}}(N_2,N_1|n_2,n_1) . \tag{50d}$$

These are shown in Fig. 3.

The first [Fig. 3(b)] is obtained by interchanging corresponding input and output states via a mirror reflection about the physical (x,y) axes of the beam splitter, and by invoking time reversal. The second [Fig. 3(c)] interchanges noncorresponding input and output states by a reflection about the diagonal $y=-x$ and time reversal. The third symmetry [Fig. 3(d)] interchanges the input and output states among themselves simply by effecting a reflection about the diagonal $y=x$ without time reversal. Only two of the three symmetries are independent, for the third can be obtained by operating with the first two in succession. These symmetries will be useful when we present specific beam-splitter output distributions.

Finally, from the last of the symmetries of Eq. (50d), and with further use of Eq. (49), we find that

$$P_{\text{out}}(N_2,N_1|n_1,n_2) \rightarrow P_{\text{out}}(N_1,N_2|n_1,n_2) \quad \text{if } \tau \rightarrow 1-\tau . \tag{50e}$$

The marginal photon-number distribution at the second output port can then be readily obtained from that of the first output port by interchanging the beam-splitter transmittance τ and reflectance $(1-\tau)$.

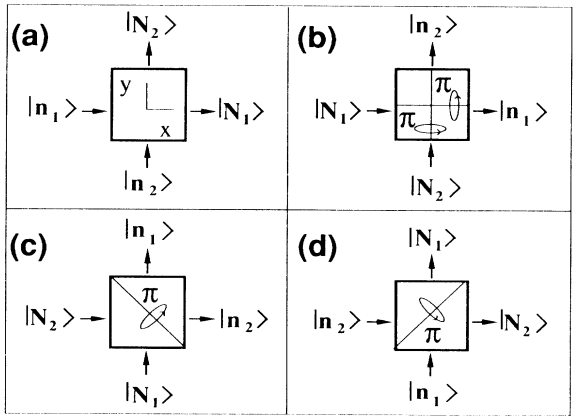

FIG. 3. Three physical symmetries are intrinsic to number-state photomixing with the unitary beam splitter. The standard beam-splitter configuration is shown in (a), where we define reference (x,y) axes and the sense of the arrows is understood as a time coordinate t. The standard configuration is equivalent to (b) by mirror reflections and time reversal, $(-x,-y,-t)$, to (c) by left-diagonal reflection and time reversal, $(-y,-x,-t)$, and to (d) by right-diagonal reflection without time reversal, (y,x,t). Energy conservation requires that $n_1+n_2=N_1+N_2$.

D. Photomixing with the vacuum

Consider those input states for which a vacuum field is present at either port, i.e.,

$$|n_1,0\rangle, \quad |0,n_2\rangle \ . \tag{51}$$

These have maximal projection of the angular momentum ($m=\pm l$), so that the action of the ladder operators of Eq. (24b) ceases,

$$\hat{L}_{\pm}|l,\pm l\rangle=0 \ . \tag{52}$$

Aside from a trivial phase factor, the beam-splitter operator of Eq. (25) displaces these states of maximal projection of angular momentum via Eq. (26a) to generate the Bloch [or SU(2) coherent] state,[26,27]

$$|\zeta\rangle_{\pm l}=\hat{D}(\zeta)|l,\pm l\rangle \ . \tag{53}$$

The Bloch states are completely equivalent to the generalized binomial field states[28,29] at the beam-splitter output ports, since the output photon-number probability amplitudes then reduce to

$$R^{(n_1,0)}_{N_1,n_1-N_1}=(-1)^{n_1-N_1}\left[\binom{n_1}{N_1}\tau^{N_1}(1-\tau)^{n_1-N_1}\right]^{1/2}, \tag{54a}$$

$$R^{(0,n_2)}_{N_1,n_2-N_1}=\left[\binom{n_2}{N_1}(1-\tau)^{N_1}\tau^{n_2-N_1}\right]^{1/2} . \tag{54b}$$

The binomial probability distributions resulting from Eq. (47b),

$$P_{\text{out}}(N_1,n_1-N_1|n_1,0)=\binom{n_1}{N_1}\tau^{N_1}(1-\tau)^{n_1-N_1} , \tag{54c}$$

$$P_{\text{out}}(N_1,n_2-N_1|0,n_2)=\binom{n_2}{N_1}(1-\tau)^{N_1}\tau^{n_2-N_1} , \tag{54d}$$

are of particular interest because they can be derived solely from classical considerations. Each input photon, behaving as a classical particle, independently undergoes a Bernoulli trial (coin toss) at the beam splitter. The fluctuations in photon number given by Eq. (41) can then be obtained simply by using the cascade variance theorem,[30,31]

$$\begin{aligned}\text{var}(\hat{N}_1)&=\tau^2\text{var}(\hat{n}_1)+\tau(1-\tau)\langle\hat{n}_1\rangle\\&=\tau(1-\tau)n_1 \quad \text{for } |n_1,0\rangle \ ,\\ \text{var}(\hat{N}_1)&=(1-\tau)^2\text{var}(\hat{n}_2)+\tau(1-\tau)\langle\hat{n}_2\rangle\\&=\tau(1-\tau)n_2 \quad \text{for } |0,n_2\rangle \ .\end{aligned} \tag{55}$$

Beam-splitter experiments with the vacuum have indeed demonstrated binomial counting statistics.[6] For a general joint input state with a vacuum at either port, Eq. (44) provides the well-known binomial sampling theorem.[30–32]

E. Interference in the photon-number domain

We now move toward an interpretation of the output photon-number probability amplitude by recasting Eq. (48a), with the aid of Eqs. (54a) and (54b), into the form

$$R^{(n_1,n_2)}_{N_1,N_2}=\sum_{k=0}^{n_1}\left[\binom{N_1}{k}\binom{N_2}{n_1-k}\right]^{1/2} \times R^{(n_1,0)}_{k,n_1-k}R^{(0,n_2)}_{N_1-k,n_2-N_1+k} \ . \tag{56}$$

This expression provides the relationship for the output photon-number probability amplitude, when number states are incident on both ports, in terms of the results for photomixing with the vacuum. Equation (56) represents a superposition of product binomial amplitudes that govern the classical selection of k out of n_1 photons from the first input beam and N_1-k out of n_2 photons from the second input beam, at the first output port. The weights of this sum are themselves binomial coefficients, reflecting excess shufflings within the set of N_1 photons at the first output port (as well as of the remaining $N_2=n_1+n_2-N_1$ photons at the second output port). The alternating signs of the successive terms of Eq. (56), hidden in the first binomial amplitude, govern the effects of constructive and destructive interference in the photon-number domain. The square of Eq. (56) provides the probability of observing N_1 photons at the first output port and N_2 photons at the second output port.

We now present some specific examples of number-state photomixing. The quantity l represents half the total number of photons at both input ports, so that $l=\frac{1}{2}$ implies that there is only a single photon in the system, as shown in Fig. 4. The vacuum must therefore exist at one or the other input port; the simple Bernoulli photon-number distribution therefore results, in accordance with Eqs. (54c) and (54d). Interference in the photon-number distribution is not present for this value of l.

In Fig. 5 we present analytical expressions and graphical results for the set of $(2l+1)=3$ possible configurations associated with $l=1$ (two photons in the system), when the beam-splitter transmittance $\tau=\frac{1}{4}$. Results for three photons in the system ($l=\frac{3}{2}$) with the same value of the transmittance are shown in Fig. 6. The distributions that result from photomixing with the vacuum are simply binomials. The others, however, are multimodal.

The symmetries of the beam-splitter number-state output probabilities are useful for understanding these distributions. The third equality in Eq. (50d), for instance, tells us that the probability distributions expected when the inputs are interchanged are just the reverse of each other, as observed in Figs. 4 and 5. This allows an economical presentation of the results for higher values of l; the mirror-image configurations need not be shown. The two distributions shown in Fig. 6 thus completely characterize the family of distributions for three photons in the system.

The first two equalities in Eq. (50d) are most interesting. Together, they show that each distribution also traces through the family the output photon-number

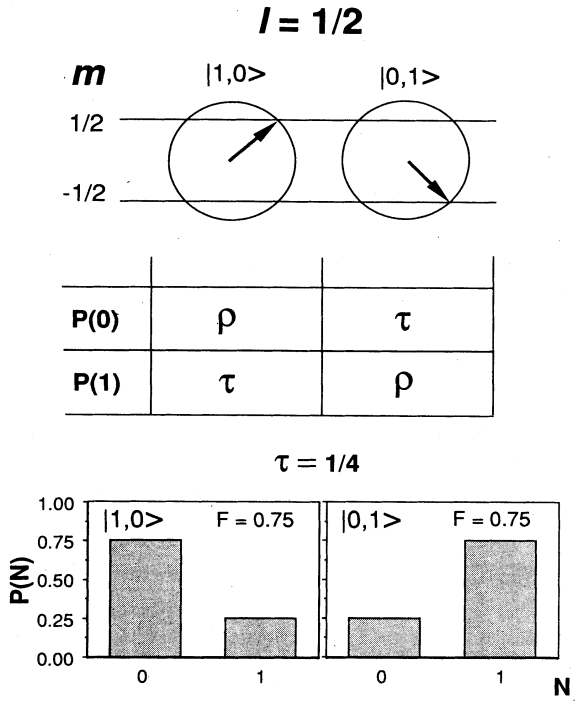

FIG. 4. Beam-splitter-output marginal photon-number probability distributions for $l=\frac{1}{2}(n_1+n_2)=\frac{1}{2}$, where n_1 and n_2 denote the number of photons at the input ports of the beam splitter (in this case there is only a single photon in the system). Each possible input ket corresponds to a projection $m=\frac{1}{2}(n_1-n_2)$ of the Schwinger angular momentum. The table displays the output marginal photon-number distribution in terms of the beam-splitter transmittance τ and reflectance $\rho=(1-\tau)$. Distributions are shown graphically for $\tau=\frac{1}{4}$. The Fano factor F, defined as the ratio of the photon-number variance to the photon-number mean, is shown in each case. The photon-number distributions are mirror images of each other.

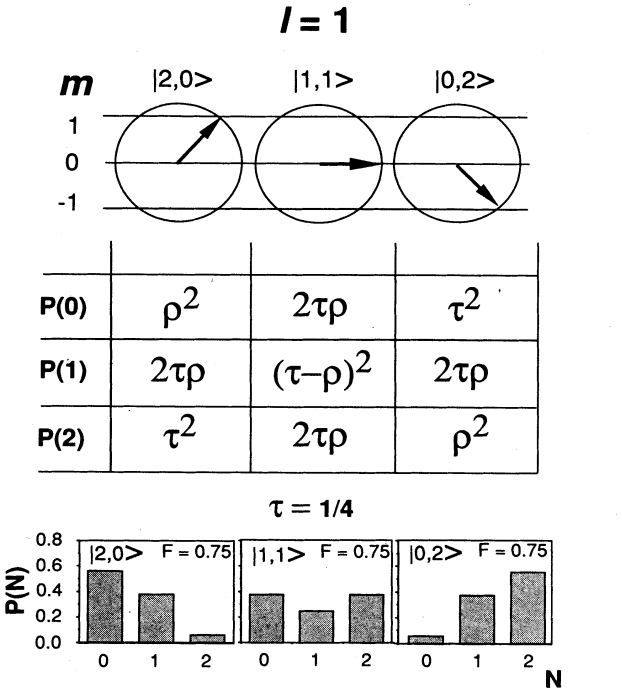

FIG. 5. Beam-splitter-output marginal photon-number probability distributions for a total of two photons at the input ports $[l=\frac{1}{2}(n_1+n_2)=1]$, when the beam-splitter transmittance $\tau=\frac{1}{4}$.

probability corresponding to its position in the family. In Fig. 5, for example, the leftmost distribution maps the evolution of the marginal probability $P_{\text{out}}(0)$ at the first output port, which, by the mirror-image property, is also the evolution of $P_{\text{out}}(2)$ in reverse. The center distribution maps $P_{\text{out}}(1)$ for the family $l=1$. The general effect of these symmetries is an interchange of the center and edge binomial probabilities, as is clear from the tables and distributions in Figs. 4–7.

The photon-number variance-to-mean ratio, or Fano factor F, provides a measure of the deviation from a Poisson photon number, which has a Fano factor of unity.[32] For number-state homodyning, from Eqs. (30), (32), and (41),

$$F=\frac{\tau(1-\tau)(n_1+n_2+2n_1n_2)}{\tau n_1+(1-\tau)n_2}\ . \tag{57}$$

The Fano factor is generally greater for nonvacuum photomixing than for photomixing with the vacuum, and for intermediate rather than small or large values of τ. The

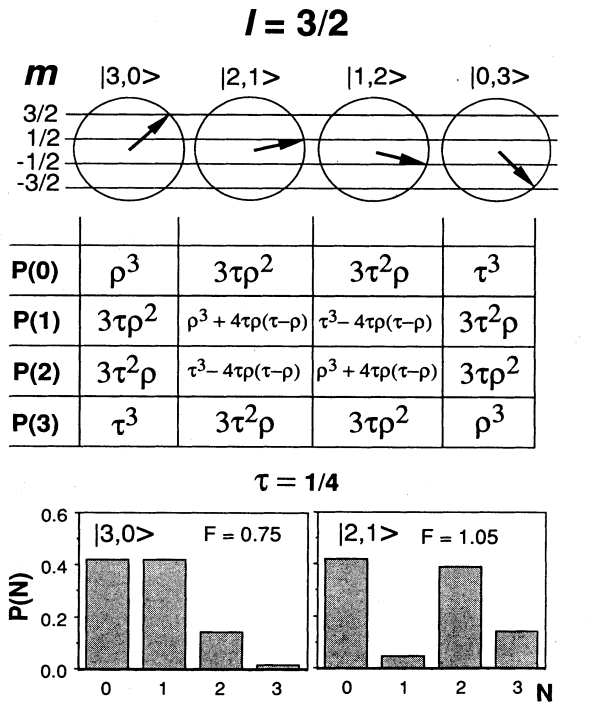

FIG. 6. Beam-splitter-output photon-number probability distributions for a total of three photons at the input ports ($l=\frac{3}{2}$), when the beam-splitter transmittance $\tau=\frac{1}{4}$. The photon-number distributions for $|1,2\rangle$ and $|0,3\rangle$ are mirror images of those shown.

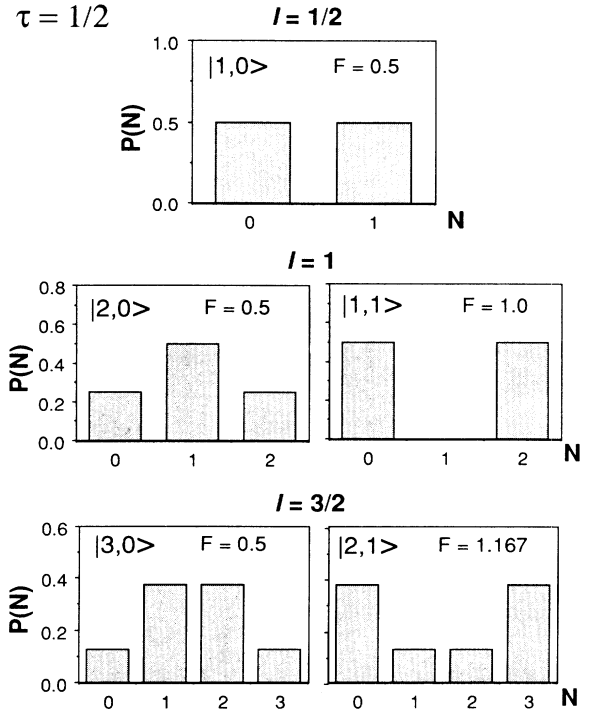

FIG. 7. Beam-splitter-output photon-number probability distributions for a total of one, two, and three photons at the input ports ($l=\frac{1}{2}$, 1, and $\frac{3}{2}$, respectively), when the beam-splitter transmittance $\tau=\frac{1}{2}$. The omitted number-state configurations are identical to those shown. Note that $P_{\text{out}}(1)=0$ when one photon is incident at each input port ($|1,1\rangle$).

Fano factors associated with the output photon-number distributions are indicated in Figs. 4–10.

The output photon-number distributions can be calculated for arbitrary input photon-number states by using a three-term recursion relation for the output photon-number probability amplitude.[33] Using the conjugate rotation of $\hat{L}_3$ via Eq. (19a) leads to

$$(2\tau-1)\hat{L}_3 e^{i2\arccos(\tau^{1/2})\hat{L}_2}-e^{i2\arccos(\tau^{1/2})\hat{L}_2}\hat{L}_3 =[\tau(1-\tau)]^{1/2}(\hat{L}_+ +\hat{L}_-)e^{i2\arccos(\tau^{1/2})\hat{L}_2}, \quad (58)$$

which, when evaluated by means of Eq. (43d) with the help of Eq. (24b), yields the desired recursion relation

$$R^{(n_1,n_2)}_{N_1,N_2}=\mu_{N_1}R^{(n_1,n_2)}_{N_1-1,N_2+1}-\nu_{N_1}R^{(n_1,n_2)}_{N_1-2,N_2+2}, \quad 2\le N_1\le n_1+n_2, \quad (59a)$$

$$\mu_{N_1}=\frac{(\tau-\frac{1}{2})[(2N_1-1)-(1+n_1+n_2)]-\frac{1}{2}(n_1-n_2)}{[\tau(1-\tau)N_1(1+n_1+n_2-N_1)]^{1/2}}, \quad (59b)$$

$$\nu_{N_1}=\left[\frac{(N_1-1)[(1+n_1+n_2)-(N_1-1)]}{N_1(1+n_1+n_2-N_1)}\right]^{1/2}, \quad (59c)$$

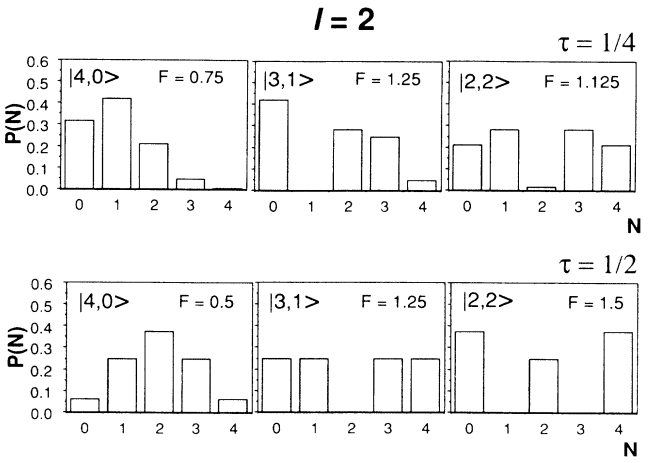

FIG. 8. Comparison of beam-splitter-output photon-number probability distributions for a total of four photons at the input ports ($l=2$), when the beam-splitter transmittance $\tau=\frac{1}{4}$ and $\tau=\frac{1}{2}$. The photon-number distributions for the input states not shown are mirror images of those shown.

together with the initial conditions

$$R^{(n_1,n_2)}_{0,n_1+n_2}=(-1)^{n_1}\left[\begin{pmatrix}n_1+n_2\\ n_1\end{pmatrix}\tau^{n_2}(1-\tau)^{n_1}\right]^{1/2}, \quad (59d)$$

$$R^{(n_1,n_2)}_{1,n_1+n_2-1}=\mu_1 R^{(n_1,n_2)}_{0,n_1+n_2}. \quad (59e)$$

The zeroth-order result was obtained directly from Eq. (48a). The algorithm is highly efficient; for high values of n_1 and n_2, Stirling's approximation can be used to generate the seed amplitude. The photon-number distribution is obtained by squaring the recursion-relation results.

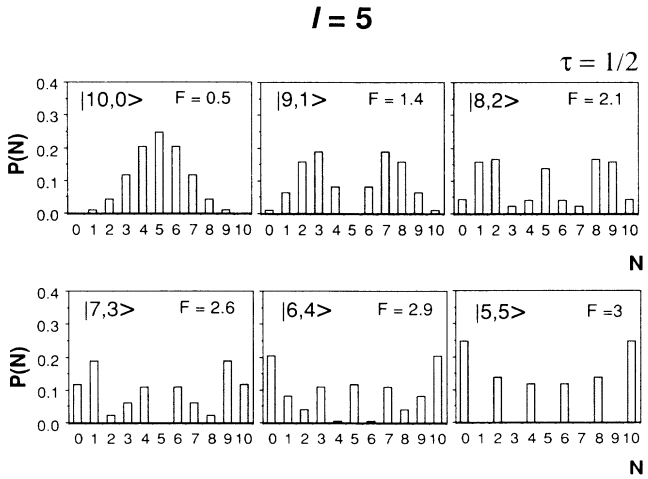

FIG. 9. Comparison of beam-splitter-output photon-number probability distributions for a total of ten photons at the input ports ($l=5$), when the beam-splitter transmittance $\tau=\frac{1}{2}$. The unimodal binomial distribution for a vacuum-state input at one port ($|10,0\rangle$) evolves into a distribution in which odd photon numbers are absent when there are equal numbers of photons at each port ($|5,5\rangle$).

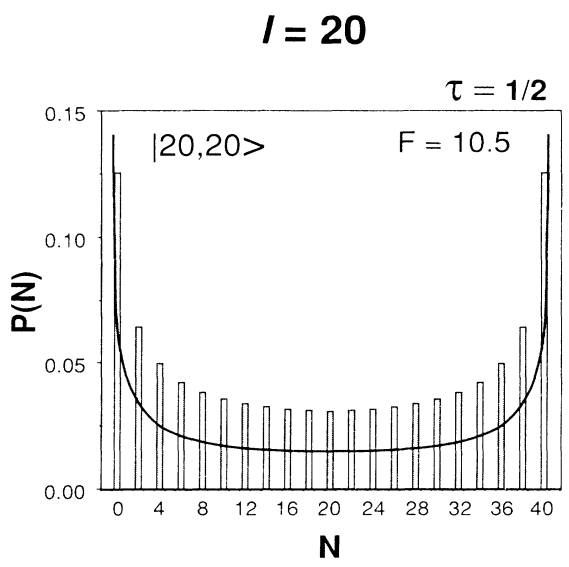

FIG. 10. Pairlike behavior of photons is always observed when the beam-splitter transmittance $\tau=\frac{1}{2}$ and $n_1=n_2$ (in this particular example, $n_1=n_2=20$). The photon-number probabilities are zero at odd-count numbers. At even-count numbers, they are nearly twice the values expected from a classical vector model (solid curve).

F. Photon-pair behavior

Finally, we turn to the input-state configuration $n_1=n_2=n$ ($m=0$), which can be realized only when the system contains an even number of photons ($l=n=$ integer). Under these circumstances, the Jacobi polynomials are proportional to the associated Legendre polynomials, and hence to the standard spherical harmonics.

The last equality of Eq. (50d) indicates that the output photon-number distribution is symmetrical in n, regardless of the value of the transmittance. This is evident for the $|1,1\rangle$ distributions in Figs. 5 and 7, the $|2,2\rangle$ distribution in Fig. 8, the $|5,5\rangle$ distribution in Fig. 9, and the $|20,20\rangle$ distribution in Fig. 10.

A number of remarkable consequences follow if we also consider a 50-50 beam splitter ($\tau=\frac{1}{2}$), as indicated in Figs. 7–10. In this case, the recursion coefficient μ_{N_1} of Eq. (59b) vanishes altogether,

$$\mu_{N_1}=0 \quad (\tau=\tfrac{1}{2},\ \ n_1=n_2=n)\ , \tag{60a}$$

so that the recursion relation in Eq. (59a) reduces to the simple form

$$R^{(n,n)}_{N_1,2n-N_1}=-\nu_{N_1}R^{(n,n)}_{N_1-2,2n-N_1+2}\ . \tag{60b}$$

The probability of observing odd photon numbers at the beam-splitter output then vanishes, as is clear from Figs. 7–10. For ten photons in the system ($l=5$), Fig. 9 displays how the binomial distribution becomes a multimodal distribution and, ultimately, evolves into a distribution that exhibits only photon pairs when five photons are incident at each input port ($|5,5\rangle$).

This result can also be obtained directly from Eq. (48a) with $\tau=\frac{1}{2}$, whereupon

$$R^{(n,n)}_{2k,2n-2k}=\left\langle 2k,2n-2k\left|\frac{[(\hat{a}_1^{\dagger})^2-(\hat{a}_2^{\dagger})^2]^n}{2^n n!}\right|0,0\right\rangle\ , \tag{61}$$

where k represents the number of output photon pairs. This form of the result arises from the vacuum by pair jumps. The outcome is surprising, inasmuch as photon-pair behavior is ordinarily associated with nonlinear parametric interactions, which are governed by the SU(1,1) group of Lorentz transformations.[8] A direct expansion of Eq. (61) provides a closed-form solution for the output photon-number probability amplitude,

$$R^{(n,n)}_{2k,2n-2k}=(-1)^{n-k}\left[\binom{2k}{k}\binom{2n-2k}{n-k}\left(\frac{1}{2}\right)^{2n}\right]^{1/2}\ ,$$

$$k=0,1,\ldots,n\ . \tag{62a}$$

With the help of Eq. (47b), the photon-number distribution then assumes the simple form

$$P_{\rm out}(2k,2n-2k|n,n)=\binom{2k}{k}\binom{2n-2k}{n-k}\left(\frac{1}{2}\right)^{2n}\ . \tag{62b}$$

Equation (62b) is known in probability theory as the fixed-multiplicative discrete arcsine law of order n.[34] It arises in the context of a one-dimensional symmetric random walk (Bernoulli trials with equal probabilities of success and failure), and provides the probability of a last return to the origin at the $2k$th Bernoulli trial, out of a finite sequence of $2n$ trials. Since an even number of trials is always required to attain a return to origin, the probability distribution must necessarily vanish for odd numbers of trials.

Comparing the discrete arcsine distribution with the binomial distribution, it is clear that the highest probabilities occur at low- and high-count numbers in the former, and near the mean-count number in the latter. The Fano factor of the discrete arcsine distribution, which can be derived from Eq. (57), has half the value associated with the Bose-Einstein distribution with mean photon number n, i.e.,

$$F=\tfrac{1}{2}(1+n),\quad n>0\ . \tag{63}$$

It is always greater than that of the binomial and other photomixing distributions with unequal numbers of photons at the two input ports (see, for example, Fig. 9).

The simplest manifestation of photon-pair behavior occurs when there is identically one photon at each input port, as shown in Fig. 7. The fact that $P_{\rm out}(1,1|1,1)$ vanishes has been theoretically predicted[5,11] and experimentally confirmed by the coincidence measurement of photomixed signal and idler photons from a parametric downconverter.[5,7] A photon-number probability distribution for high n ($|20,20\rangle$) is shown in Fig. 10. The arcsine distribution now clearly exhibits a shape that becomes increasingly well defined for larger values of n.

It is of interest to compare these results with those obtained from the classical vector model.[33] Consider a vec-

tor of azimuthal angle ϕ on the equator ($m=0$) of the angular-momentum sphere with radius $[n(n+1)]^{1/2}$ (a classical version of Fig. 2). After a rotation by 90° ($\tau=\frac{1}{2}$), the vector attains a projection

$$M=N_1-n=[n(n+1)]^{1/2}\cos\phi \ . \tag{64a}$$

Randomizing ϕ uniformly on the interval $(0,\pi)$ leads to the probability density

$$f_{N_1}(N_1)=\frac{1}{\pi}\frac{1}{[n(n+1)-(N_1-n)^2]^{1/2}} \ ,$$
$$n-[n(n+1)]^{1/2}\le N_1\le n+[n(n+1)]^{1/2} \ . \tag{64b}$$

This density can be mapped into the unit interval by effecting the transformation

$$x=\frac{1}{2}\left[1+\frac{N_1-n}{[n(n+1)]^{1/2}}\right] , \tag{65a}$$

such that

$$f_x(x)=\frac{1}{\pi}\frac{1}{[x(1-x)]^{1/2}}, \quad 0\le x\le 1 \ . \tag{65b}$$

The result is the Lévy arcsine probability density, which can be sampled to provide the discrete arcsine law with good accuracy[34]

$$P_{\rm out}(2k,2n-2k|n,n)\approx\frac{1}{n}f_x\left[\frac{k}{n}\right] . \tag{66a}$$

For large values of n, Eqs. (65a) and (66a) provide the approximation

$$P_{\rm out}(2k,2n-2k|n,n)\approx 2f_{N_1}(2k) \ . \tag{66b}$$

This is evident in Fig. 10, where Eq. (64b) is plotted as the solid curve. The approximation fails only near the end points of the photon-number distribution.

V. THE BALANCED PHOTOMIXER

In accordance with the discussion in Sec. III, photomixing is, in general, a noisy process. However, substantial noise reduction can be achieved by effecting a two-port measurement of the difference in output photon numbers, which is measured by the output angular-momentum projection operator [see Eq. (15d) with Eq. (9b)],

$$\hat{L}'_3=\tfrac{1}{2}(\hat{N}_1-\hat{N}_2)=2\{(\tau-\tfrac{1}{2})\hat{L}_3+[\tau(1-\tau)]^{1/2}\hat{I}\} \ , \tag{67a}$$

where we have employed Eq. (28) in the last step. For the 50-50 beam splitter ($\tau=\frac{1}{2}$)

$$\hat{L}'_3=\hat{I} \ , \tag{67b}$$

so the output statistics are governed solely by the interference operator, and will hence exhibit only its associated fluctuations, as per Eq. (37).

Balanced photomixing has a long history of use in homodyne as well as heterodyne optical detection with nonunity quantum efficiencies, both for eliminating local-oscillator classical fluctuations[35–37] and quantum fluctuations.[38,39] We show that for an ideal measurement this property is not predicated on the use of a coherent local oscillator, but rather holds for arbitrary input states. It is an intrinsic property of the beam splitter. In essence, the balanced mixer takes advantage of the natural anticorrelations between the interference operators at the two output ports, which differ in phase by π [see Eqs. (4e) and (28)]. This is mandated by energy conservation, and therefore SU(2) symmetry, since we must recover Eq. (9a) by summing Eqs. (28a) and (28b).

The output distribution for the balanced mixer can be easily obtained from the considerations of Sec. IV. Since we measure the output projection of angular momentum,

$$M\equiv\tfrac{1}{2}(N_1-N_2) \ , \tag{68a}$$

it then follows that, in accordance with Eq. (45a), the output distribution for the balanced mixer is given by

$$P_{\rm bal}(M)=\sum_{N_1=0}^{\infty}P_{\rm out}(N_1,N_1-2M)$$
$$=\sum_{N_2=0}^{\infty}P_{\rm out}(N_2+2M,N_2) \ . \tag{68b}$$

For number states at the input to the beam splitter, the result is particularly simple. According to Eq. (43e), we can write

$$M=N_1-l, \quad l=\tfrac{1}{2}(n_1+n_2) \ , \tag{69a}$$

so the output distribution is given by

$$P_{\rm bal}(M)=P_{\rm out}(M+l,l-M|n_1,n_2) \ . \tag{69b}$$

This is equivalent to the marginal photon-number distribution at the first output port, except that it is shifted and centered about the origin in probability space by half the total number of photons in the system (the parameter l).

ACKNOWLEDGMENTS

This work was supported by the Joint Services Electronics Program and the National Science Foundation through the Center for Telecommunications Research at Columbia University.

[1] J. Mod. Opt. **34** (No. 6/7) (1987) (special issue on squeezed light).
[2] J. Opt. Soc. Am. B **4** (No. 10) (1987) (special issue on squeezed states of the electromagnetic field).
[3] H. P. Yuen and J. H. Shapiro, IEEE Trans. Inf. Theory **IT-26**, 78 (1980).
[4] P. Grangier, G. Roger, and A. Aspect, Europhys. Lett. **1**, 173 (1986).
[5] C. K. Hong, Z. Y. Ou, and L. Mandel, Phys. Rev. Lett. **59**, 2044 (1987); Z. Y. Ou and L. Mandel, *ibid.* **61**, 54 (1988).

[6]J. Brendel, S. Schütrumpf, R. Lange, W. Martienssen, and M. O. Scully, Europhys. Lett. **5**, 223 (1988); R. Lange, J. Brendel, E. Mohler, and W. Martienssen, *ibid.* **5**, 619 (1988).

[7]J. G. Rarity and P. R. Tapster, J. Opt. Soc. Am. B **6**, 1221 (1989).

[8]B. Yurke, S. L. McCall, and J. R. Klauder, Phys. Rev. A **33**, 4033 (1986).

[9]S. Prasad, M. O. Scully, and W. Martienssen, Opt. Commun. **62**, 139 (1987).

[10]Z. Y. Ou, C. K. Hong, and L. Mandel, Opt. Commun. **63**, 118 (1987); classical reciprocity relations akin to the quantum ones [Eq. (4)] are discussed by Z. Y. Ou and L. Mandel, Am. J. Phys. **57**, 66 (1989).

[11]H. Fearn and R. Loudon, Opt. Commun. **64**, 485 (1987); H. Fearn and R. L. Loudon, J. Opt. Soc. Am. B **6**, 917 (1989).

[12]B. Huttner and Y. Ben-Aryeh, Phys. Rev. A **38**, 204 (1988).

[13]P. Jordan, Z. Phys. **94**, 531 (1935).

[14]J. Schwinger, U.S. Atomic Energy Commission Report. No. NYO-3071 (U.S. GPO, Washington, D.C., 1952); reprinted in *Quantum Theory of Angular Momentum*, edited by L. C. Biedenharn and H. van Dam (Academic, New York, 1965).

[15]H. Goldstein, *Classical Mechanics*, 2nd ed. (Addison-Wesley, Reading, MA, 1980).

[16]U. M. Titulaer and R. J. Glauber, Phys. Rev. **145**, 1041 (1966).

[17]G. Baym, *Lectures on Quantum Mechanics* (Benjamin-Cummings, Reading, MA, 1969).

[18]L. C. Biedenharn and J. D. Louck, *Angular Momentum in Quantum Physics: Theory and Application, Encyclopedia of Mathematics and its Applications* (Addison-Wesley, Reading, MA, 1981), Vol. 8.

[19]I. M. Gel'fand, R. A. Minlos, and Z. Ya. Shapiro, *Representations of the Rotation and Lorentz Groups and their Applications* (Pergamon, Oxford, 1963) (translated from Russian by G. Cummins and T. Boddington).

[20]The Baker-Hausdorff lemma for the transformation of $\hat{Y}$ via some Hermitian $\hat{X}$ reads

$$e^{-i\hat{X}}\hat{Y}e^{i\hat{X}}=\hat{Y}-i[\hat{X},\hat{Y}]+\frac{i^2}{2!}[\hat{X},[\hat{X},\hat{Y}]]-\cdots .$$

[21]B. L. Schumaker, Phys. Rep. **135**, 317 (1986).

[22]R. J. Glauber, Phys. Rev. **130**, 2529 (1963); **131**, 2766 (1963).

[23]D. F. Walls, Am. J. Phys. **45**, 952 (1977).

[24]*Handbook of Mathematical Functions*, National Bureau of Standards Applied Mathematics Series No. 55, edited by M. Abramowitz and I. A. Stegun (U.S. GPO, Washington, D.C., 1964).

[25]W. Magnus, F. Oberhettinger and R. P. Soni, *Formulas and Theorems for the Special Functions of Mathematical Physics* (Springer-Verlag, New York, 1966).

[26]J. M. Radcliffe, J. Phys. A: Gen. Phys. **4**, 313 (1971).

[27]F. T. Arecchi, E. Courtens, R. Gilmore, and H. Thomas, Phys. Rev. A **6**, 2211 (1972).

[28]D. Stoler, B. E. A. Saleh, and M. C. Teich, Opt. Acta **32**, 345 (1985).

[29]G. Dattoli, J. Gallardo, and A. Torre, J. Opt. Soc. Am. B **4**, 185 (1987).

[30]J. Peřina, *Quantum Statistics of Linear and Nonlinear Optical Phenomena* (Reidel, Dordrecht, Holland, 1984).

[31]M. C. Teich and B. E. A. Saleh, Opt. Lett. **7**, 365 (1982); J. Peřina, B. E. A. Saleh, and M. C. Teich, Opt. Commun. **48**, 212 (1983).

[32]M. C. Teich and B. E. A. Saleh, in *Progress in Optics*, edited by E. Wolf (North-Holland, Amsterdam, 1988), Vol. 26, pp. 1–104.

[33]E. de Prunelé, J. Math. Phys. **29**, 2523 (1988).

[34]W. Feller, *An Introduction to Probability Theory and its Applications*, 3rd ed. (Wiley, New York, 1968), Vol. I.

[35]T. Waite and R. A. Gudmundsen, Proc. IEEE **54**, 297 (1966); T. Waite, *ibid.* **54**, 334 (1966).

[36]H. Van der Stadt, Astron. Astrophys. **36**, 341 (1974).

[37]G. L. Abbas, V. W. S. Chan, and T. K. Yee, J. Lightwave Tech. **LT-3**, 1110 (1985).

[38]H. P. Yuen and V. W. S. Chan, Opt. Lett. **8**, 177 (1983); **8**, 345(E) (1983); B. L. Schumaker, *ibid.* **9**, 189 (1984).

[39]S. Machida and Y. Yamamoto, IEEE J. Quant. Electron. **QE-22**, 617 (1986).